Chapter 4
Transducers' Range Modeling

4.1 Introduction

Transducers have been proposed for many unattended surveillance applications, forest fire detection, and healthcare monitoring. As we use a thermometer to measure temperature, the reading represents for the whole body and there is no need to use a second thermometer. Thus, the body area represents sensing range of a thermometer transducer. So, in most common applications, each transducer represents that parameter for a given area and it is said to detect events within its *sensing range* . The event could include presence of fire, presence of an animal, or no. of soldiers, or tanks or flow of oxygen. Transducers collaborate other functional units of a SN to deliver data to processing centre commonly known as a base station (BS or sink node) via one or more intermediate SNs. Many previous works assume *disk* sensing model [1] wherein a transducer is assumed to accurately indicate value of sensed parameter in a circular area of radius r_s (Fig. 4.1a) and do not have any knowledge outside the area as shown in Fig. 4.1b. A laser transducer emits laser beam transducer in a linear form and is illustrated in Fig. 4.2a, and a digital camera coverage area is in the form of a fan as shown in Fig. 4.1b. The wiggle effect shown in Fig. 4.2c confirms the fact that nothing is perfect in the world and exact location of the transducer may not be accurate. So, still assuming circular sensing area, the circle wiggles at the exact location of the transducer. The area covered by a transducer is simply approximated by a wiggle from its central location.

Additional area covered by the wiggle effect of an *i*th transducer may have error w_i. Let disk radius be represented by *X and* wiggle radius *y as an* (*X*, *y*) *disk.* Then, an (*R*, *w*) disk is functionally equivalent to an (*R*–*w*, 0) disk. For any point *P of distance greater than R–w from the center of the* disk *O, there exists a point Q whose distance from O is less than w and whose distance* from *P* is greater than *R*. Point *P* is not covered if the center of the disk is on *Q*, and it is better to take an intersection of the two sensing ranges: normal range and wiggle range and are

D.P. Agrawal, *Embedded Sensor Systems*,
DOI 10.1007/978-981-10-3038-3_4

illustrated in Fig. 4.4. 1-D wiggle basically takes error in one dimension, say x; while 2-D wiggle incorporates error in both x and y dimensions (Fig. 4.3).

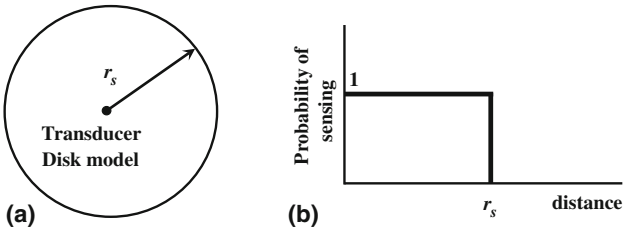

Fig. 4.1 **a** Disk model of a transducer and **b** probability of sensing by a transducer

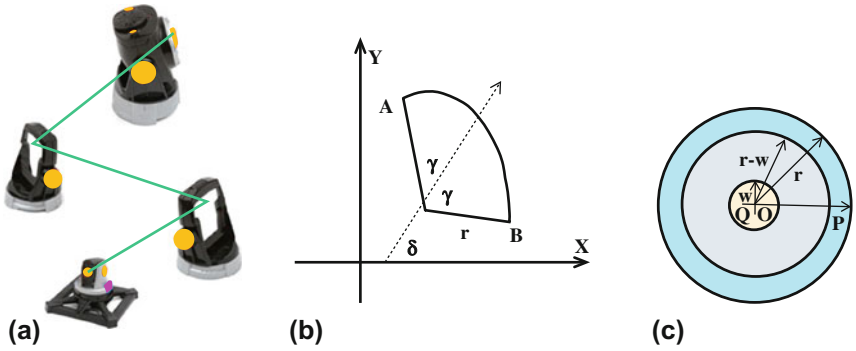

Fig. 4.2 **a** Linear segment of a laser transducer [2], **b** Fan model of a camera transducers, and **c** Wiggle effect of a disk model for a transducer

Fig. 4.3 **a** Sensing range of a transducer, **b** sensing range of a transducer with 1-D giggle, and **c** sensing range of a transducer with 2-D giggle [3]

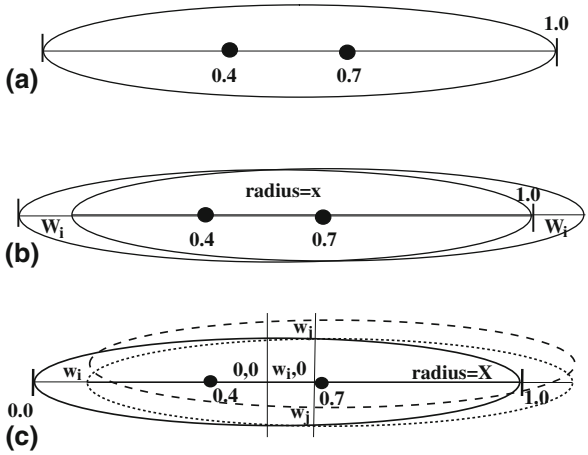

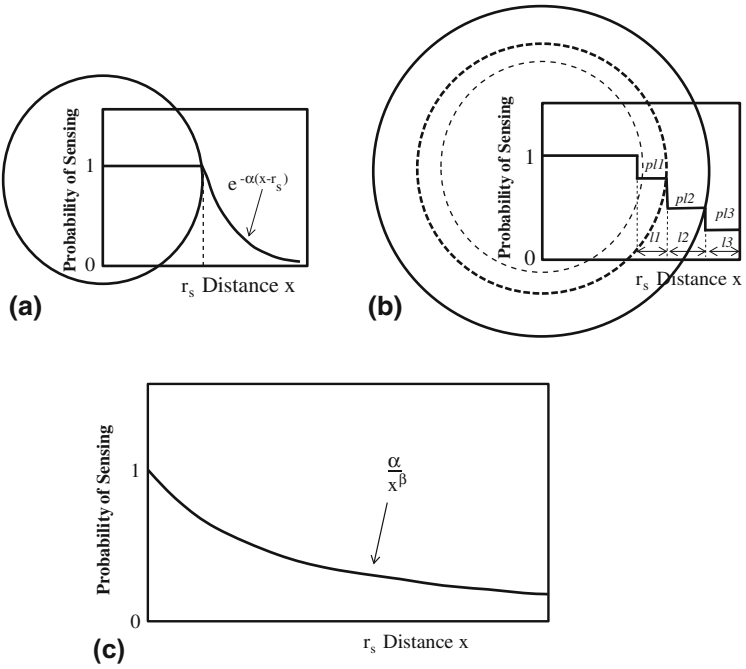

Fig. 4.4 Three sensing range models of a transducer **a** Zou et al. [4], **b** Ahmed et al. [5], and **c** Liu et al. [7]

4.2 Modeling of a Transducers' Sensing Range

Disk sensing model of a transducer is being used as it is easier to design and analyze coverage area while it is not realistic [4–6]. For example, you take a temperature of a child and an adult and tend to use body area as the sensing coverage area of the thermometer transducer that varies drastically. Moreover, nothing is perfect in the world and saying that the transducer can only represent of an area r_s and cannot say beyond r_s is rather incorrect as we are measuring physical parameter of an environment where value is expected to change slowly and rather smoothly. Moreover, signals do not fall abruptly and there are fair chances that the transducer will estimate the event parameter beyond r_s. So, many other models have been suggested in the literature and three most important ones are shown in Fig. 4.5.

A major assumption in disk model is that if an event occurs at a distance up to r_s, the transducer will correctly record and represent occurrence of the event and will be detected. The disk sensing model of a transducer is appealing as it is simple and less complicated to analyze and simulate. However, it is quite unlikely that physical signal will drop abruptly from full value to zero and there is some chance to detect an event at distance greater than r_s from the transducer. Thus, a disk model does not

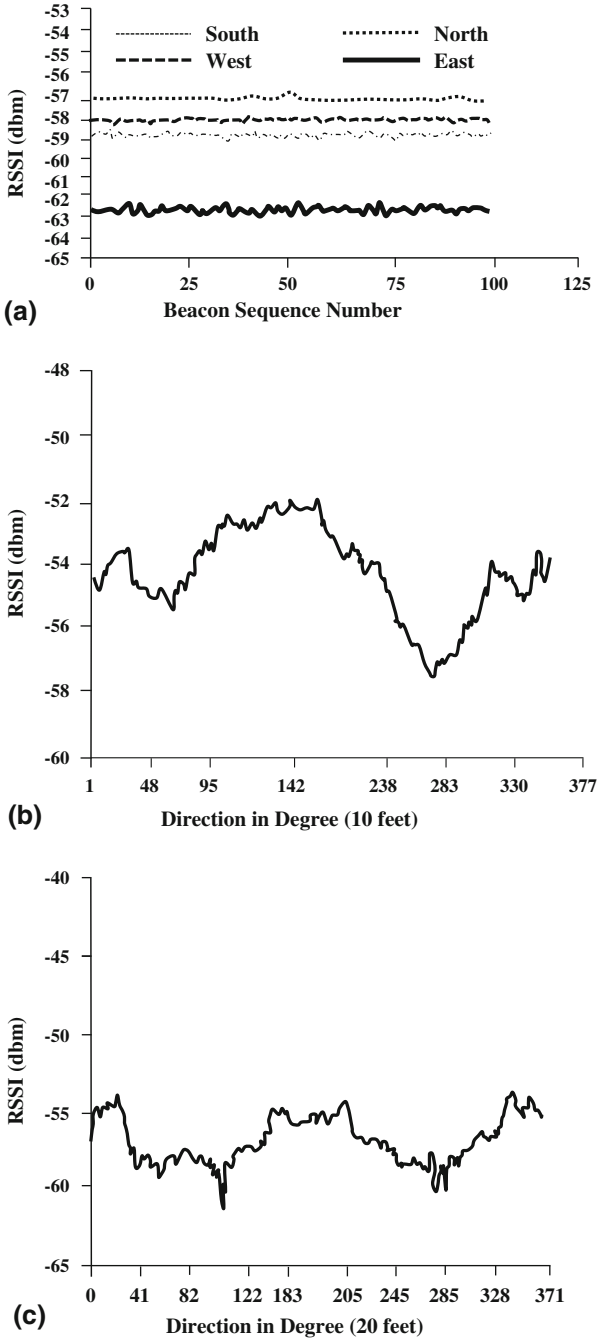

Fig. 4.5 **a** Signal strength in 4 directions as a function of time, **b** received signal strength (RSSI) measured at 10 feet, and **c** received signal strength (RSSI) measured at 20 feet [9]

fully utilize transducers' sensing ability and more transducers may be deployed than needed, requiring more money. The redundant transducers cause increased interference and waste energy. In the first model [4], the probability of sensing correctly up to r_s distance is assumed to be 1 and then decays exponentially. In the second model, a step function is used and the probability of correctly predicting sensed parameter is assumed to be fixed (<1 for distance larger than r_s) for different ranges. In the third model, the probability of correctly measuring the parameter varies exponentially with distance of point from the transducer.

A probabilistic sensing model of a transducer is assumed to realistic as the parameter being sensed the transducer design and the ecological settings are stochastic in nature. Identical SNs and transducers do not exhibit exactly identical behavior, and sensing range of transducers no longer follows nice regular disks. A probabilistic coverage (PCP) model has been proposed [8] wherein no single sensing model can accurately model different transducer types and the surrounding environment could impact the results. Simulation results indicate that PCP outperforms other schemes in terms of transducer (SN) requirements and energy consumption and robust against random failure and imprecise location determination and inaccurate synchronization. In PCP, an area is covered by all n-deployed transducers collectively. The least-covered probability θ of a point in a given subarea is the centre of three transducers forming a triangle, and the maximum separation between any two transducers dictate the number of SNs and transducers needed. PCP has been implemented PCP [8] using ns-2 for up to 1000 nodes. Later on up to 20,000 nodes deployed in a 1 km × 1 km area.

Characteristics of different types of transducers are summarized in Table 4.1. In most applications, disk model is adopted. But, radio propagation follows anisotropic diffusion (nonlinear) process and the value changes continuously, even with a small change in the direction. A pair of MICA motes is used [9] to observe such

Table 4.1 Characteristics of different types of transducers [9]

Transducer type	Data rate	Sensing range	Sensing power	Coverage shape
Temperature/humidity	Low	Short	Low	Disk
Vibration	High	Short	Low	Disk
Pressure	Low	Short	Low	Disk
Microphone	High	High	High	Disk
Smoke detector	Low	Long	Low	Disk
Accelerometer	High	Short	Low	Disk
Radiation	Low	Long	Low	Disk
Scanner	High	Short	High	Disk
Motion using accelerometer	Low	Long	High	Disk
Infrared laser tripwire	High	Short	High	Line segment
Camera	High	Long	High	Fan
Motion using camera	Low	Short	Low	Fan
Magnetic	Low	Short	Low	Fan
Electrical Field	Low	Short	Low	Fan

irregular variations in received signal strength, packet reception ratio, and communication range and is shown in Fig. 4.5a. Thus, the radio irregularity is a common phenomenon and it is hard to neglect. Variation in the signal strength in different directions also affects the packet loss rate.

Irregularity is present, indicating different communication ranges (Fig. 4.6. RSS threshold is selected between −55.5 and −59 dBm. dBm could be written more completely as dBmW (Fig. 4.7).

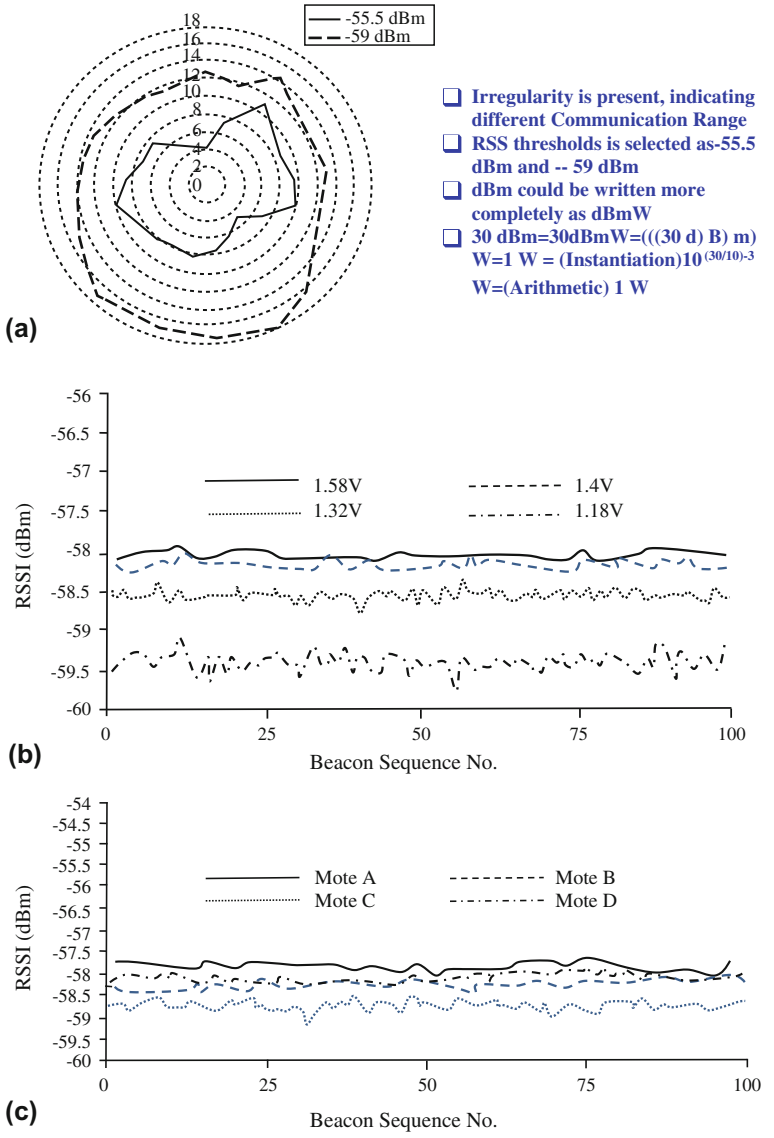

Fig. 4.6 **a** Anisotropic ratio range, **b** one mote with different battery status, and **c** many motes with the same battery status [9]

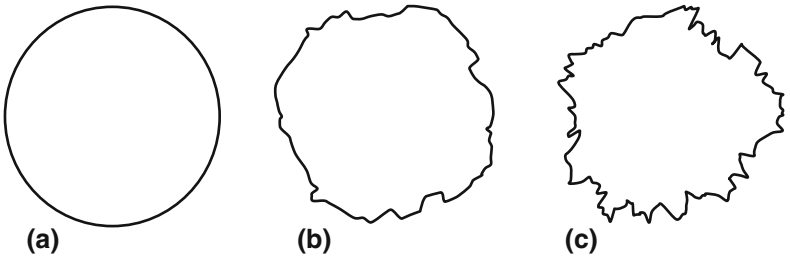

Fig. 4.7 **a** Degree of irregularity = 0, **b** degree of irregularity = 0.003, and **c** degree of irregularity = 0.01 [9]

Battery power level (Fig. 4.8a) does not remain fixed and does not fit a normal distribution. SNs are divided into two groups: sentry SNs and non-sentry SNs. Sentry SNs are supposed to work all the time. Non-sentry SNs are put to sleep to save power and are only awakened when an important event occurs. The degree of irregularity (DOI) assumes an upper and lower bounds on signal propagation. RIM (radio irregularity model) takes into account radio sending energy, energy loss, background noise, and interference among different communication signals. Figure 4.9b, c show

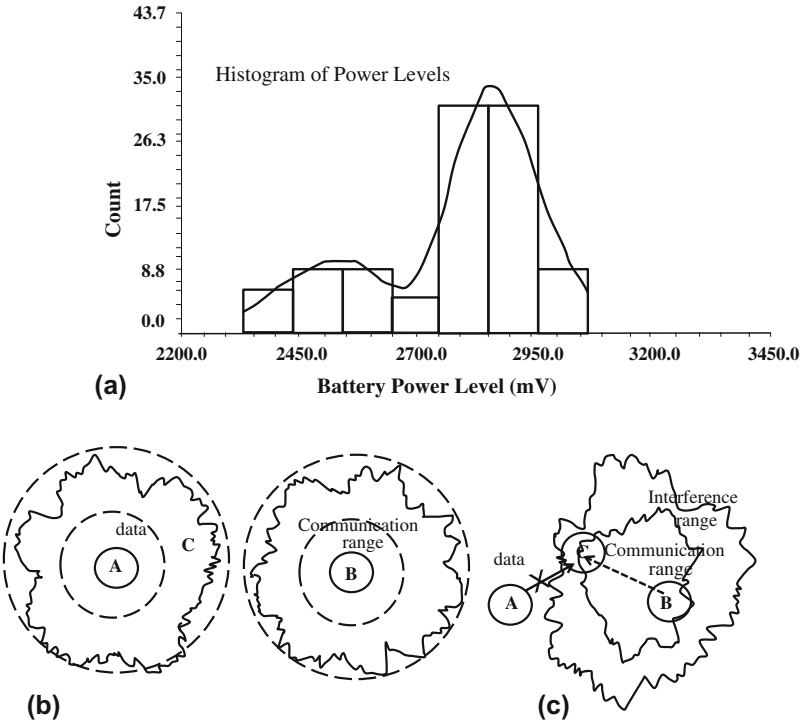

Fig. 4.8 **a** Battery power snapshot, **b** no interference in DOI, and **c** interference in radio irregularity model [9]

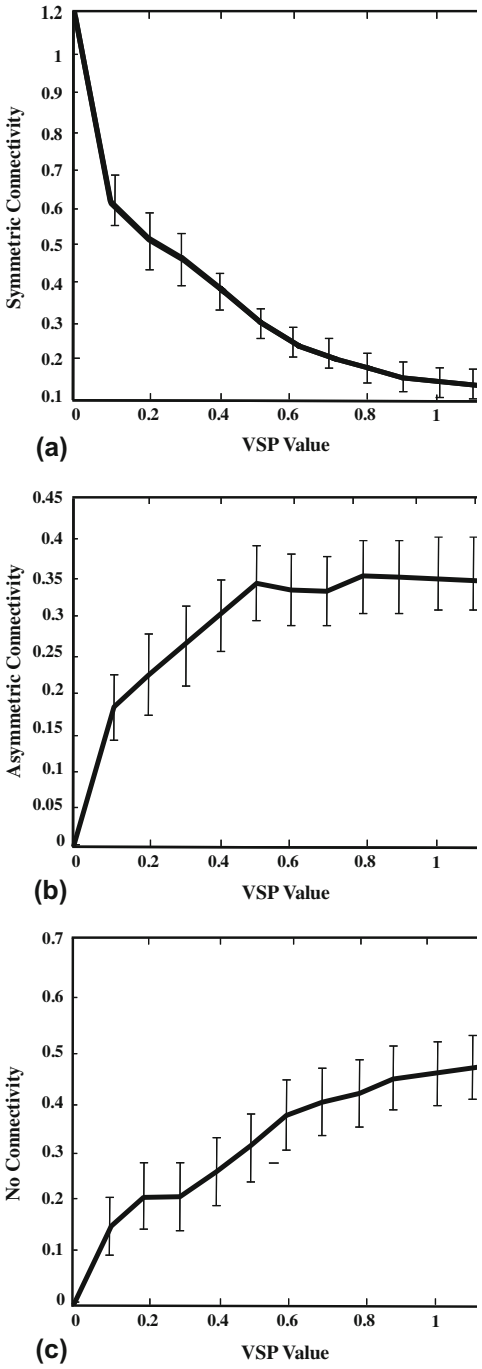

Fig. 4.9 **a** Impact of topology with symmetric connectivity, **b** impact of topology with asymmetric connectivity, and **c** impact of topology with no connectivity [9]

the impact of communication interference. Geographical adaptive fidelity (GAF) is also considered as a function of symmetric, asymmetric, and no connectivity (Fig. 4.9) between adjacent SNs in a terrain divided into virtual grids, and in each grid, one SN remains awake while others sleep to save power.

Many transducers exhibit directional properties such as measuring sound with voice, wind speed, direction mass airflow, wind direction, traffic counting, vibration, tilt, occupancy, directional LEDs, pressure, heat and temperature. The corresponding sensing area of a directional transducer SN under the disk and sector models is shown in Fig. 4.10. A directional sensing area approximated by the polygon model is shown in Fig. 4.11a. The sensing range is approximated by a set of nodes $[(R_1, q_1)\ldots(R_i, q_i)\ldots(R_x, q_x)]$, where R_i is the distance of i**th** node from the SN and q_i is counterclockwise angle. The calculation of $R_s(S_n, P_i)$ under the polygon model (Fig. 4.11b) can be given by the sensing range of S_n in the direction of P_i that can be given by:

$$R_s(S_n, P_i) = \frac{\left(R_{sp} \cdot R_{sq}\right) \times \sin\left(\theta_{sq} - \theta_{sp}\right)}{R_{sp} \times \sin\left(\theta(s_n, P_i) - \theta_{sp}\right) - R_{sq} \times \sin\left(\theta(s_n, P_i) - \theta_{sq}\right)}, \tag{4.1}$$

where $q_{\text{sp}} < q(S_n, P_{i)} < q_{sq}$, $R_s(S_n, P_{i)} = d(P_a, P_j)$, and P_j is the intersection point of ray $P_a{\cdot}P_j$ and line segment vex_p and vex_q. The sensing coverage level (SCL) of a SN S_n that can be used by topology control mechanism (Fig. 4.11c) is given by:

$$\text{SCL}(S_n, P_i) = [R_s(S_n, P_i)/d(S_n, P_i)]^2 \tag{4.2}$$

The sensing range S_n in the direction P_i can be given by:

$$R_s(S_n, P_i) = \frac{\left(R_{sp} \cdot R_{sq}\right) \times \sin\left(\theta_{sq} - \theta_{sp}\right)}{R_{sp} \times \sin\left(\theta(s_n, P_i) - \theta_{sp}\right) - R_{sq} \times \sin\left(\theta(s_n, P_i) - \theta_{sq}\right)} \tag{4.3}$$

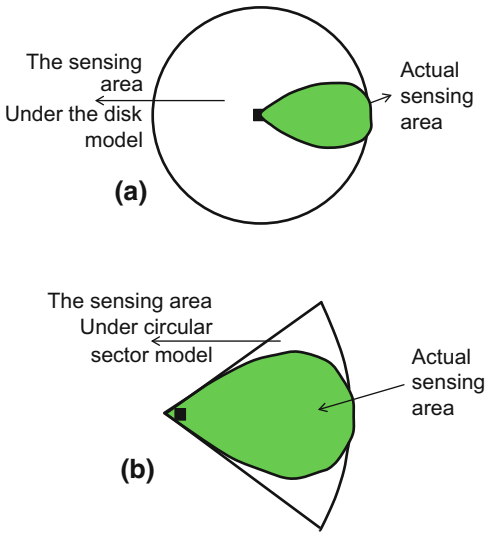

Fig. 4.10 **a** Sensing area of a directional transducer and **b** sensing area of a circular sector directional transducer [10]

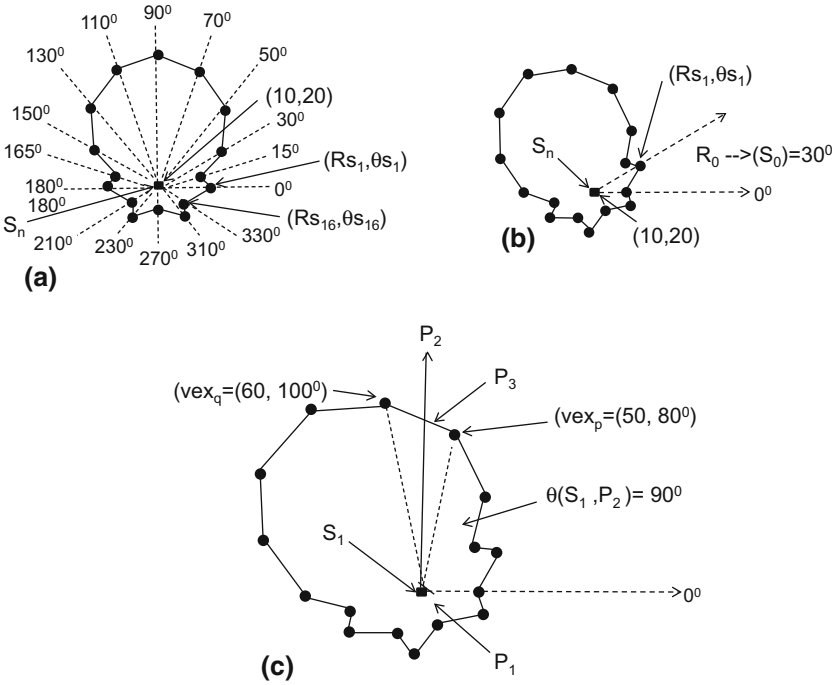

Fig. 4.11 **a** Directional sensing area by the polygon model, **b** directional sensing area approximated by the polygon model, and **c** calculation of sensing coverage range $R_s(S_n, P_i)$ [10]

This is plotted in Fig. 4.12. If $d(S_n, P_i) \leq R_s(S_n, P_i)$, P_i is within the sensing area of S_n. Otherwise, it cannot be covered by sensing area of S_n. In case of obstacles, the calculation of the CCL (communication coverage level) and SCL follows the "line-of-sight" property.

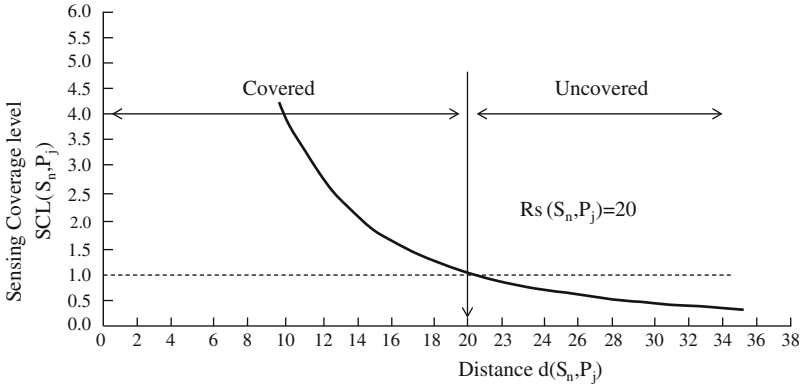

Fig. 4.12 Relationship between sensing coverage level and distance from S_n [10]

Table 4.2 Subdivisions of IR [12]

Division name	Abbreviation	Wavelength (μm)	Frequency (THz)	Photon energy (meV)
Near-infrared	NIR, IR-A*DIN*	0.75–1.4	214–400	886–1653
Short-wavelength infrared	SWIR, IR-B*DIN*	1.4–3	100–214	413–886
Mid-wavelength infrared	MWIR, IR-C*DIN*; MidIR. also called intermediate infrared (IIR)	3–8	37–100	155–413
Long-wavelength infrared	LWIR, IR-C*DIN*	8–15	20–37	83–155
Far-infrared	FIR	15–1000	0.3–20	1.2–83

In most applications, disk-type model is used except in few cases where either infrared beam is used to have point-to-point communication or camera with pixel-based transducers is used in a camera SN (C-SN) to provide a fan-type coverage. Infrared (IR) is invisible radiant electromagnetic energy that has longer wavelength of 700 nm to 1 mm (frequency 430 THz to 300 GHz) than visible light [11]. It is worth mentioning that most thermal radiation by objects in room temperature is IR. IR is commonly divided into the schemes shown in Table 4.2.

Near-IR is defined by water absorption in fiber optical communication. Water absorption increases to 1450 nm in short-wavelength IR while 3–5 μm band is used in mid-wavelength IR missiles. The thermal imaging provides complete image of objects in long-wavelength IR. The IR communication band is divided [13] as shown in Table 4.3.

C is the dominant band for long-distance communication networks while S and L bands are not widely deployed. IR is also employed in short-range communication between peripherals by LEDs where a beam is switched off and on to encode data. IR cannot penetrate walls but does not interfere with other devices. IR lasers operate in 4 gigabits/s in urban areas. Strong IR in high temperature could be harmful to eyes.

Table 4.3 Telecommunication bands in IR [13]

Band	Descriptor	Wavelength range (nm)
O band	Original	1260–1360
E band	Extended	1360–1460
S band	Short wavelength	1460–1530
C band	Conventional	1530–1565
L band	Long wavelength	1565–1625
U band	Ultra-long wavelength	1625–1675

4.3 Modeling of Camera Transducers' (C-SN) Sensing Range

A digital camera (C-SN) is a solid-state system that captures light and converts through a viewfinder or LCD monitor into an image and an equivalent of a film [14]. Received image can be manipulated or scaled. Characterizing parameters of a C-SN are image size, resolution, low-light performance, depth of field, dynamic range, lenses, and physical size. Smaller C-SN utilizes crop factor to lenses, capturing less of a scene. In that way, sensing range is limited while a large number of transducers can be considered to be present in a camera. So, the problem in such transducer is not the sensing model but the orientation of the camera coverage area. The most common C-SNs are CCD (charge-coupled device) and CMOS (complementary metal–oxide–semiconductor). The largest size C-SN is called a full frame (36 mm × 24 mm), and larger sensor has a bigger body. Active pixel sensor (28.7 mm × 19 mm) is the most popular type with fixed and interchangeable lens. 17.3 mm × 13 mm is a quarter-sized camera. 1 inch (13.2 mm × 8 mm) camera is a pocket-sized camera with a crop factor larger than 2.7. Smartphones such as iPhone 5 employ 1/3 inch (4.8 mm × 3.6 mm) lens. Thus, a camera can be said to be equivalent to have a large number of transducers, with each transducer sensing only one pixel area among millions of pixels.

The pixel size in digital C-SN is affected by the dynamic range defined as maximum signal divided by noise floor in a pixel which is a combination of noise, A/D conversion limitations, and amplifier noise. The number of pixels impacts the image quality than single pixel [15]. So, the problem with C-SN is different from a SN transducer and the sensing area/range for a given C-SN is pretty much fixed. So, the problem with C-SN is different from SN as a large number of C-SNs are deployed and their orientation given in Fig. 4.13b plays an important role in determining overall sensing area.

Figure 4.13a shows two randomly deployed C-SNs in a 10 × 10 grid area and can be calculated by diving the area into small grids and then the coverage c can be defined as:

$$c = \frac{\text{Number of covered grids}}{\text{Number of total grids}}, \tag{4.4}$$

$$c = \frac{20}{100} = 0.2. \tag{4.5}$$

An area C covered with N random C-SNs is shown in Fig. 4.13b and can be expressed as:

$$c = 1 - \left(1 - \frac{\alpha R^2}{S}\right)N, \tag{4.6}$$

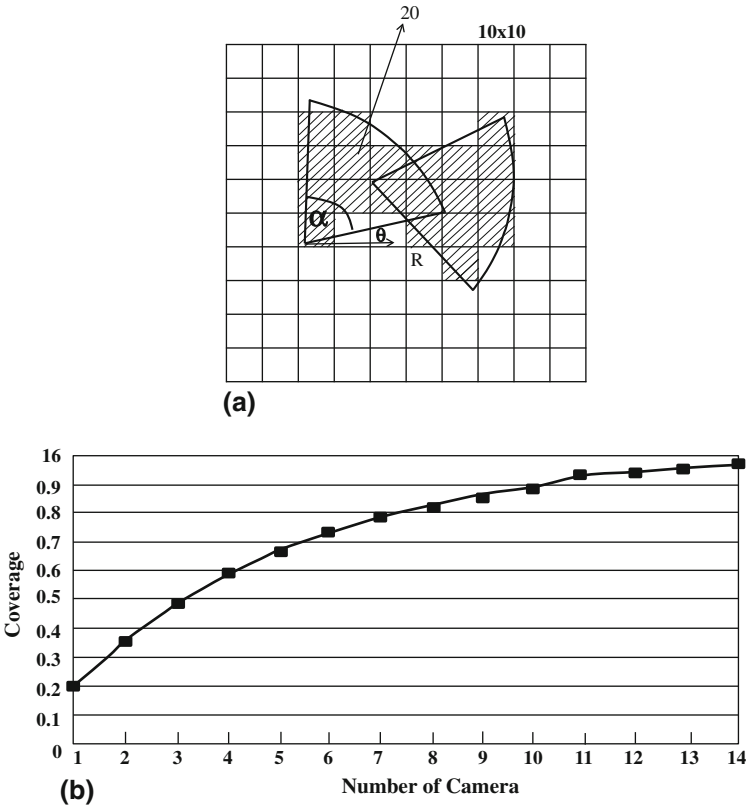

Fig. 4.13 **a** Two C-SNs and coverage area and **b** coverage area as a function of randomly deployed C-SNs

where R is the radius of area covered and α coverage angle.

In other words, given c, N, the number of desired C-SNs can be given by:

$$N = \frac{\ln(1-c)}{\ln(S - \alpha R^2) - \ln S}. \tag{4.7}$$

Coverage area as a function of number of C-SNs is given in Fig. 4.13b. The first 7 cameras can increase the coverage to 0.8 from zero, but the next 7 C-SNs can only improve the coverage by only 0.16. Each C-SN cannot change its position but can change its orientation, and reports that to the controlling station. A simple optimization problem is to determine orientations $(\theta_1, \theta_2, \theta_3, \ldots, \theta_n)$ such that the coverage is maximized. This is done by using a particle swarm organization (PSO) algorithm that uses M particles, with each particle having position vector x and velocity vector v; *remembering a private best position p for each particle, global best g is obtained by doing iterations by following two steps:*

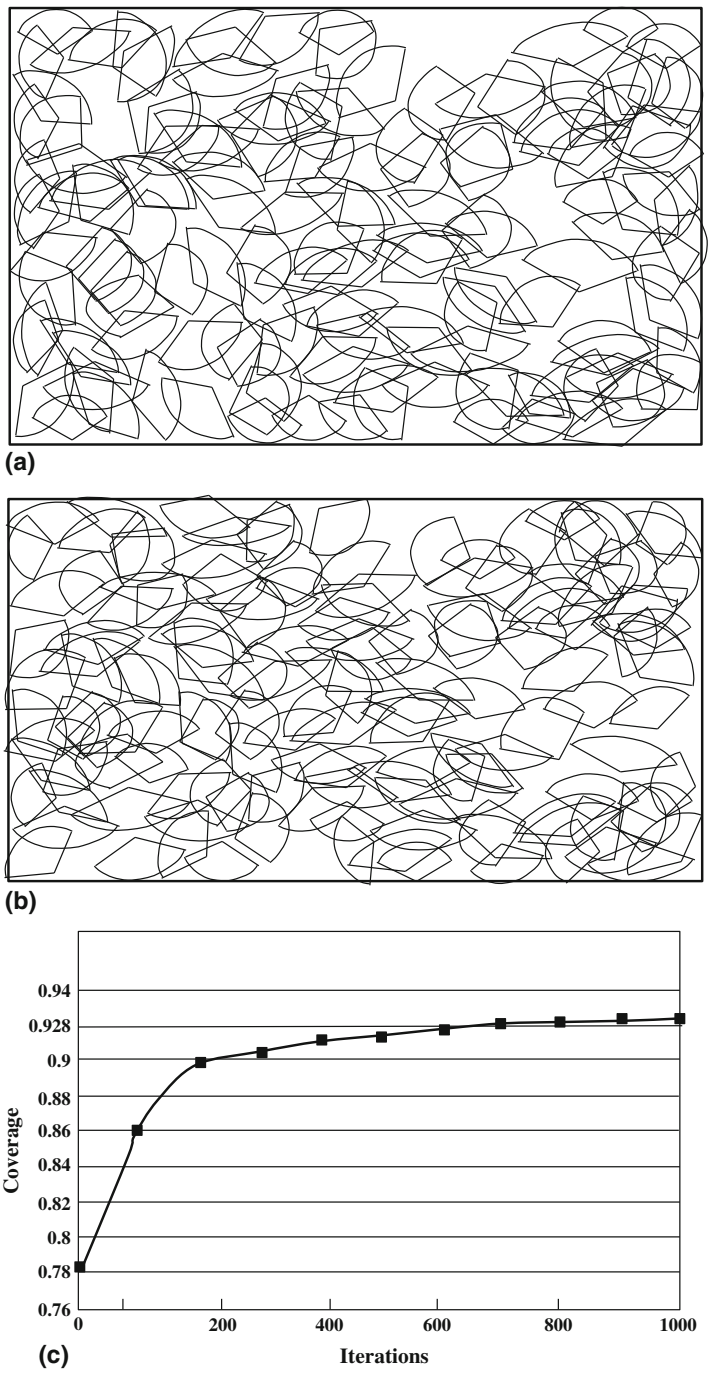

Fig. 4.14 **a** Initial layout of 152 C-SNs with *coverage of 0.782052*, **b** improved layout of 152 cameras to *0.92336*, and **c** variations of coverage with iterations

$$\begin{aligned} v &= C_1 \times v + C_2 \times \text{rnd}() \times (p - x) + C_3 \times \text{rnd}() + (g - x) \\ x &= x + v \end{aligned}, \tag{4.8}$$

where C_1, C_2, and C_3 are constants. Based on prior work [16], we set $C_1 = 0.729$, $C_2 = C_3 = 1.49445$. In an experiment, 500 × 500 rectangular area is monitored with 152 randomly distributed C-SNs, with each having $R = 50$, $\alpha = \pi/3$. 20 particles are used with maximum iteration = 1000. The global best coverage of 0.782052 is improved to 0.92336 after 1000 iterations (14% improvement) which will require 244 C-SNs if no orientation improvement is applied (Fig. 4.14).

4.4 Conclusions

As transducer plays a very important role in numerous applications, it is important to model the same appropriately. Precisely, modeling makes the simulation and analysis more accurate but also helps in minimizing required number of SNs. The challenge is to define a good model that is simple enough to be used while leading to reasonable results in a time effective manner.

4.5 Questions

Q.4.1. What is meant by modeling of a transducer sensing range?
Q.4.2. How do I test my sensor to make sure it is working properly?
Q.4.3. What is the role of noise in a transducer?
Q.4.4. Do transducers require calibration?
Q.4.5. How do you select the right transducer/sensor range for your application?
Q.4.6. Do you need a computer to use these transducers?
Q.4.7. How do thermal modeling by snake help infrared reception?
Q.4.8. How much rain does your sensor need to shut off the sprinklers?
Q.4.9. Which metrics do you use to compare transducer models for localization?
Q.4.10. Why isn't your camera sensing up to 50 feet as advertised?
Q.4.11. What are the effects of temperature on piezoceramic transducers?
Q.4.12. Why do you need to have a breath alcohol tester?
Q.4.13. What type of maintenance is required to maintain a personal house monitoring unit?
Q.4.14. What are the advantages of ultrasonic level transducers?
Q.4.15. What is the impact of coverage area if you have 10% wiggle distance?
Q.4.16. How much difference you have if you have 2-D wiggle in problem 3.14?
Q.4.17. What is the impact of irregularity on transducer coverage area?

Q.4.18. Can you envision usefulness of irregularity in helping reduce the number of transducers required to cover a given area?

Q.4.19. What will be the impact if wiggle is also present with irregularity in sensing area?

References

1. https://books.google.com/books?isbn=1849960593.
2. http://144.206.159.178/FT/CONF/16438452/16438496.pdf.
3. Amotz Bar-Noy, Theodore Brown, Matthew P. Johnson, and Ou Liu, "Cheap or Flexible Sensor Coverage," Eds.): DCOSS 2009, LNCS 5516, pp. 245–258, Springer-Verlag Berlin Heidelberg 2009.
4. Yi Zou and Krishnendu Chakrabarty, "Sensor Deployment and Target Localization Based on Virtual Forces," INFOCOM 2003, pp. 1293–1303.
5. N. Ahmed, S. S. Kanhere, and S. Jha, "Probabilistic Coverage in Wireless Sensor Networks," 30th Anniversary. The IEEE Conference on Local Computer Networks, 2005, pp. 681–688.
6. G. Wang, G. Cao, T. L. Porta, and W. Zhang, "Sensor relocation in Mobile Sensor Networks," IEEE INFOCOM'05, vol. 4, 2005, pp. 2302–2312.
7. Liping Liu, Guidan Li, Zhi Wang, and Yu-geng Sun, "Energy-Efficient Collaborative Target Coverage in Wireless Sensor Networks," Computer Engineering and Applications, Dec.2008, vol. 44, no. 34, pp.:31–34.
8. Mohamed Hefeeda and Hossein Ahmadi, "A Probabilistic Coverage Protocol for Wireless Sensor Networks," https://www.cs.sfu.ca/~mhefeeda/…/icnp07.pdf.
9. G. Zhou, T. He, S. Krishnamurthy, and J. A. Stankovic, "Models and Solutions for Radio Irregularity in Wireless Sensor Networks," ACM Transactions on Sensor Networks, vol. 2, no. 2, pp. 221–262, 2006.
10. Chun-Hsien Wu and Yeh-Ching Chung, "A Polygon Model for Wireless Sensor Network Deployment with Directional Sensing Areas," Sensors, vol. 9, pp. 9998–10022, 2009.
11. R Mulligan and A. Ammari, "Coverage in Wireless Sensor Networks: A Survey," Network Protocols and Algorithms, 2010, vol. 2, no. 2, pp. 27–53 and http://en.wikipedia.org/wiki/Radio-frequency_identification.
12. https://en.wikipedia.org/wiki/Infrared.
13. Rajiv Ramaswami, "Optical Fiber Communication: From Transmission to Networking" (PDF). IEEE Communications Magazine, vol. 40, no. 5, May 2002.
14. http://www.techhive.com/article/2052159/demystifying-digital-camera-sensors-once-and-for-all.html.
15. http://www.clarkvision.com/articles/digital.sensor.performance.summary/.
16. Yichun Xu and Bangjun Lei, "Particle swarm optimization to improve the coverage of a camera network," *Proc. SPIE* 7497, MIPPR 2009: Medical Imaging, Parallel Processing of Images, and Optimization Techniques, 749718 October 30, 2009.